ChemPubSoc Europe

DOI: 10.1002/cphc.201900340

CHEMPHYSCHEM Articles

Comparison between Hydrogen and Halogen Bonds in Complexes of 6-OX-Fulvene with Pnicogen and Chalcogen Electron Donors

Mingchang Hou,[a] Qingzhong Li,*[a] and Steve Scheiner*[b]

Quantum chemical calculations are applied to complexes of 6-OX-fulvene (X=H, Cl, Br, I) with ZH_3/H_2Y (Z=N, P, As, Sb; Y=O, S, Se, Te) to study the competition between the hydrogen bond and the halogen bond. The H-bond weakens as the base atom grows in size and the associated negative electrostatic potential on the Lewis base atom diminishes. The pattern for the halogen bonds is more complicated. In most cases, the halogen bond is stronger for the heavier halogen atom, and pnicogen electron donors are more strongly bound than chalcogen. Halogen bonds to chalcogen atoms strengthen in the order O < S < Se < Te, whereas the pattern is murkier for the pnicogen donors. In terms of competition, most halogen bonds to pnicogen donors are stronger than their H-bond analogues, but there is no clear pattern with respect to chalcogen donors. O prefers a H-bond, while halogen bonds are favored by Te. For S and Se, I-bonds are strongest, followed Br, H, and Cl-bonds in that order.

1. Introduction

Non-covalent interactions are of great importance in molecular recognition,[1] supramolecular chemistry,[2] and material science,[3] which has motivated researchers to find and understand novel types of non-covalent interactions. Hydrogen bonding (HB) is one of the most important non-covalent interactions, and the most mature.[4–6] The halogen bond (XB) represents another important interaction, with similar properties and applications to the HB, and has gained a great deal of research interest in recent years.[7–12] In general, non-covalent interactions can be thought of as Lewis acid-base interactions. In the study of halogen bonds, Clark et al,[13] used the concept of a "σ-hole" to explain the formation of a halogen bond and later to other types of non-covalent interactions. The σ-hole can be defined as a positive molecular electrostatic potential (MEP) region centered along an extension of the R–X axis. On the other hand, both HBs and XBs also have a covalent contribution due to intermolecular orbital interactions.[14] XBs have been utilized in synthesis of organic conductive electrical materials,[15–17] crystal engineering,[18] self-assembly.[19,20] The XB also plays a key role in biological molecules and as a potential tool in drug design.[21.22]

Due to the extensive applications of non-covalent interactions, the competition,[23] cooperation[24] and coexistence[25] among them have generated extensive research. It is especially important to study the competition between hydrogen bonds and halogen bonds, as these two types of interactions are directional and relatively strong, and their importance in crystal engineering originates from their shared dependence upon long-range electrostatic forces].[26–30] By combining interactions that do not compete for the same molecular binding sites it is, in principle, possible to avoid or at least minimize "synthon cross-over"[31] thereby producing architectures of considerable complexity.[32–35] Moreover, it is well known that hydrogen bonding plays an important role in the human body; for example, human DNA structure is highly dependent upon hydrogen bonds. Also, it has been demonstrated that the Holliday junction, which is an intermediate formed during homologous recombination of DNA, is stabilized through the O···Br XB interaction, whereas the hydrogen-bonded isomer is not formed.[36]

There are many factors that can regulate the competition between HB and XB, e.g. solvent polarity. This competition can be influenced by choice of solvent (polarity) to direct the self-assembly of co-crystals. Formation of hydrogen-bonded co-crystals is favored in less polar solvents and halogen-bonded co-crystals by more polar solvents.[37] Cooperativity also affects the competition between HB and XB. For example, the presence of magnesium bonding has a positive synergistic effect on the strength of HB and XB, but the enhancing effect on both interactions is different.[38] Of course, whether it is HB or XB, its strength depends mainly on the properties of Lewis acid and Lewis base. Therefore, many studies have been conducted on the effects of Lewis acid and Lewis base on the competition between HB and XB.[39–42] Herrebout et al.[39] used infrared and Raman spectra to study the HB and XB complexes formed by trimethylamine (TMA), dimethyl ether (DME) and methyl fluoride (MF) with CHF_2I. They found that both HB and XB are present in the complexes TMA···CHF_2I and DME···CHF_2I, while only XB is present in the MF···CHF_2I complex. In another work

[a] Dr. M. Hou, Q. Li
Laboratory of Theoretical and Computational Chemistry and
School of Chemistry and Chemical Engineering
Yantai University, Yantai 264005(China)
Fax: (+86)535-6902063
E-mail: li70316@sohu.com
[b] Prof. S. Scheiner
Department of Chemistry and Biochemistry
Utah State University, Logan, UT 84322–0300 (USA)
E-mail: steve.scheiner@usu.com

Supporting information for this article is available on the WWW under https://doi.org/10.1002/cphc.201900340

by Herrebout, it was found that only HB exists in the TMA···CHF_2Br complex, indicating that the transition from I to Br greatly reduces the strength of the halogen bond.[40] Although the competition for HB and XB has attracted widespread attention, there remain a number of open questions. Moreover, most of the previous studies focused mainly on the competition between HB and XB formed by the same molecule. We turn our focus here to the competition between HB and XB within different molecules.

In this work, we chose 6-OX-fulvene (X=H, Cl, Br, I) as the Lewis acid and ZH_3 (Z=N, P, As, Sb) and H_2Y (Y=O, S, Se, Te) as the Lewis bases. Both molecules can be bonded by a HB or XB when X is a hydrogen atom or a halogen atom. Fulvene is not only a precursor for the synthesis of natural compounds, [43,44] but also a starting material for the synthesis of novel substituted titanium-based biometallic organic anticancer drugs.[45] Therefore, fulvene has an important potential application in medicine and biology. Structurally, being an isomer of benzene, it is a conjugated system having an extracyclic double bond. Although fulvene is non-aromatic, it can be converted into an aromatic structure by substitution at the 6-position, and its aromaticity has also attracted widespread attention.[46] Therefore, we chose fulvene derivatives to participate in the formation of HB and XB. We selected hydrides of V and VI group atoms as Lewis bases to study the effects of different Lewis bases on the strength of hydrogen bonds and halogen bonds. Through this study, we hope to generate a better understanding of the nature of HB and XB and the influence of Lewis acid and Lewis base on the strength of both interactions.

Computational Methods

All calculations were performed using the Gaussian 09 program.[47] Geometries were optimized at the MP2 computational level with the aug-cc-pVDZ basis set for all atoms except I, Sb, and Te atoms, for which the aug-cc-pVDZ-PP basis set, with its relativistic corrections, was adopted. Frequency calculations at the same level confirmed that the structures obtained correspond to energetic minima since no imaginary frequencies were observed. The interaction energy was calculated by the supermolecular method involving the energies of the monomers at the geometries they adopt within the complex. This quantity was corrected for the basis set superposition error (BSSE) by the counterpoise protocol proposed by Boys and Bernardi.[48]

Using the nature bond orbital (NBO) method[49] within the Gaussian 09 program, charge transfer and second-order perturbation energy were obtained. The AIM2000 package[50] was used to assess the topological parameters at each bond critical point (BCP) including electron density, its Laplacian, and energy density. Molecular electrostatic potentials (MEPs), and their extrema, were calculated on the 0.001 au isodensity surface at the MP2/aug-cc-pVDZ level using the WFA-SAS program.[51] The localized molecular orbital-energy decomposition analysis[52] was used to decompose the interaction energy into five terms of electrostatic, exchange, repulsion, polarization, and dispersion at the MP2/aug-cc-pVDZ level with the GAMESS program.[53]

2. Results and Discussion

2.1. Geometries and Energetics of Complexes

Figure 1 illustrates the MEPs of 6-OX-fulvene and two types of Lewis bases (ZH_3 and H_2Y). A red region of positive MEP occurs

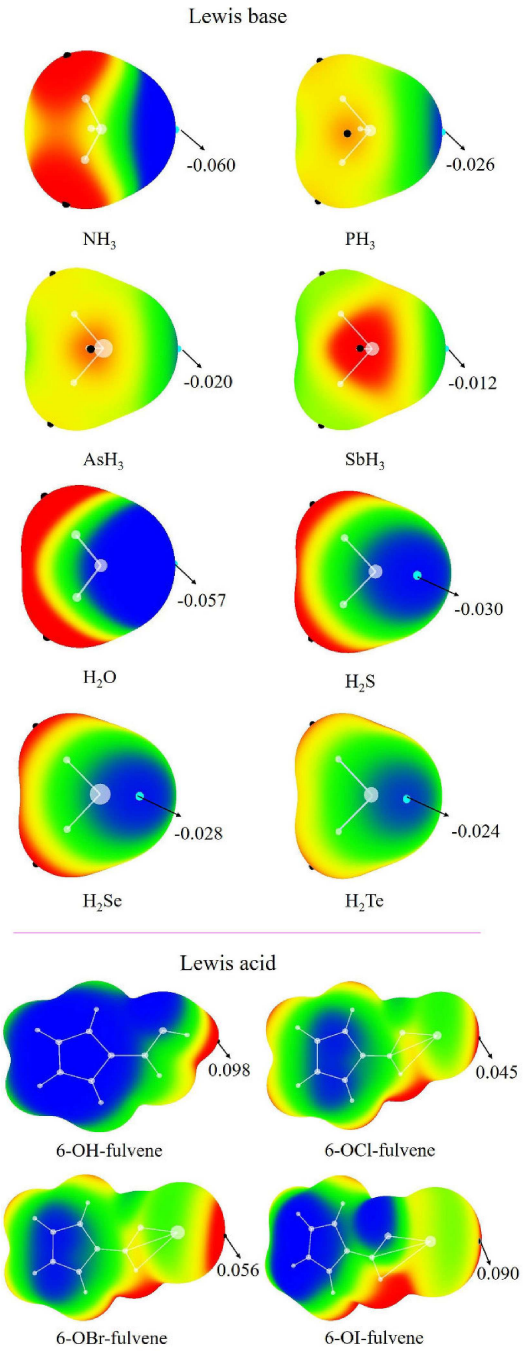

Figure 1. MEP diagrams of the Lewis acids and bases. Color ranges, in a.u., are: red, greater than 0.020; yellow, between 0.020 and 0; green, between 0 and −0.020; blue, less than −0.020. Arrows refer to values of maxima and minima.

Table 1. Interaction energies (E_{int}, kcal mol^{-1}) in the HB and XB complexes.

	E_{int}		E_{int}		E_{int}		E_{int}
H-N	−11.57	Cl-N	−7.79	Br-N	−12.32	I-N	−15.60
H-P	−4.86	Cl-P	−11.55	Br-P	−11.46	I-P	−12.46
H-As	−4.15	Cl-As	−7.80	Br-As	−9.88	I-As	−10.99
H-Sb	−3.24	Cl-Sb	−13.02	Br-Sb	−11.39	I-Sb	−11.12
H-O	−8.00	Cl-O	−3.74	Br-O	−5.49	I-O	−7.59
H-S	−4.96	Cl-S	−3.47	Br-S	−5.60	I-S	−7.60
H-Se	−4.68	Cl-Se	−3.82	Br-Se	−6.50	I-Se	−8.40
H-Te	−4.27	Cl-Te	−11.00	Br-Te	−9.80	I-Te	−10.31

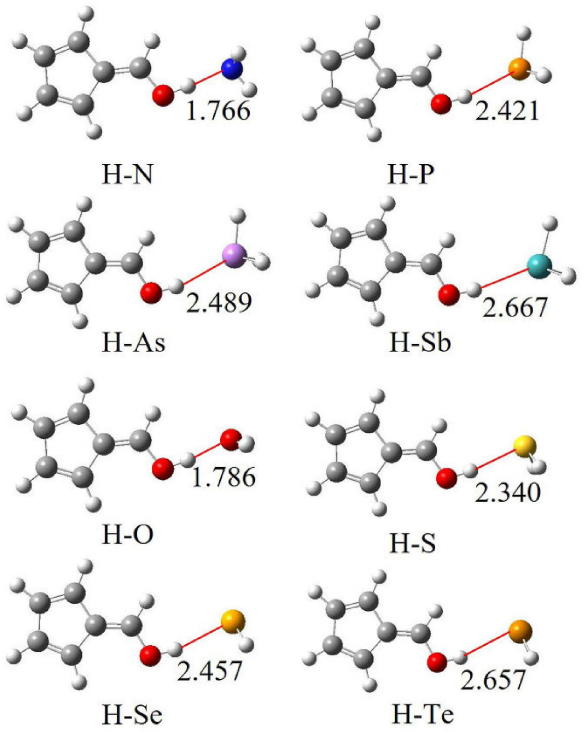

Figure 2. The optimized structures of the HB complexes (distances are in Å).

along the extension of the OH/OX bond in 6-OH-fulvene and its halogenated derivatives. The intensity of this so-called σ-hole rises in the OCl < OBr < OI < OH sequence. Regarding the various Lewis bases, a blue or green area of negative MEP is observed in the lone pair area of the Z/Y atom of ZH_3 and YH_2. The magnitude of the minimum is largest for first-row atoms N and O, then drops for succeeding rows of the periodic table. It is more negative for chalcogen than pnicogen atoms, with the exception of NH_3/OH_2 where it is the pnicogen atom that has a slightly more negative minimum.

The optimized structures of the HB complexes shown in Figure 2 display the anticipated nearly linear OH···Y/Z arrangement, which is essentially duplicated for the XB dimers that are illustrated in Figure S1 in the Supporting Information. The notation for each complex shows first the H or X atom on the fulvene, followed by the Y/Z atom of the base with which it is interacting. There are only very minor inconsistencies from one structure to the next. For example, one of the H atoms of NH_3 lies opposite the C to which the OH is connected in H–N whereas it is more of a cis orientation for the other pnicogen atoms. There is also a diminishing OH···Y linearity as the Y atom grows in size. The H/X···Y/Z intermolecular distance is shortest for the H-bonded systems, consistent with the small size of the bridging H. This distance elongates along with the size of the acceptor Y/Z atom. With regard to the H-bonds, this length is slightly greater for the pnicogen than for the chalcogen atoms, with the exception of NH_3 vs OH_2. It is the bonds to the chalcogen acceptors that are longer in the cases of the XBs. In general, the binding distance elongates for the same X donor atom as the acceptor atom grows in size although there are one or two exceptions. For example, R(Cl···Te) distance is quite a bit shorter than R(Cl···Se) due to the stronger orbital interaction in the Cl–Te complex as seen in the following section.

The interaction energies (E_{int}) of the various complexes displayed in Table 1 cover the broad range between 3 and 16 kcal/mol. The HB quantities are largest for first-row N and O acceptors, with the others much smaller, diminishing slowly as the acceptor atom grows larger. The XB dimers obey rather different trends, not necessarily consistent from one X atom to the next. For example, the strongest Cl-bonds are formed by the heaviest Sb and Te acceptor atoms, and the pnicogen complexes are consistently stronger than their chalcogen counterparts. For the case of the I-bonds, it is the lightest N pnicogen that forms the strongest bond, but the heaviest chalcogen for which this is true.

Within the context of the HB systems, E_{int} rises steadily along with the Lewis base V_{min}. Their linear relationship is displayed in Figure S2 with correlation coefficients of 0.985 and 0.999 for the ZH_3 and H_2Y bases, respectively. This close correlation is consistent with the notion that electrostatics provide a guiding factor in these HB complexes.

The sometimes erratic patterns within the larger picture of these energetics may perhaps be best understood visually through the graphic presentation of Figure S3. Beginning with the pnicogen bonds in Figure S3a, the interaction energy for AsH_3 rises steadily from H to Cl, and then to Br and I. However, the other ZH_3 molecules do not behave this simply. In the cases of PH_3 and SbH_3, the H-bond is also the weakest, but there is disagreement as to which halogen bond is strongest. It is the Cl-bond that is strongest for SbH_3, but the I-bond for PH_3. There is a clear Cl < Br < I order for NH_3, but its H-bond is stronger

than Cl, and is by far the strongest of the H-bonds considered here. The latter behavior of the H-bond repeats itself for the chalcogen electron donors in Figure S3b, with first-row H_2O replacing NH_3. All of the chalcogen donors, with the exception of TeH_2, follow a strengthening halogen bond order of Cl < Br < I, whereas TeH_2 finds the Cl-bond stronger than any other. Given the different orders for H, Cl, Br, and I-bonds, the interaction energies are clearly dependent upon factors other than simply the magnitude of V_{min} on the base.

It is known that chlorine is a mediocre halogen donor in most cases, when compared to its heavier congeners. However, when 6-OCl-fulvene binds with SbH_3 and H_2Te, they form a strong halogen bond. In a previous study, it was found that HBe and H_2B radicals bind very strongly with ClF, resulting in Cl transfer from ClF to the radical.[54] For the given Br donor, the XB interaction energy is more negative in the sequence $AsH_3 < SbH_3 \approx PH_3 < NH_3$, while the energetics pattern is the reverse of that of $V_{s,min}$ on H_2Y. A similar reverse change is also found for the IB complexes with YH_2.

Turning next to a comparison between HB and XB interactions, XBs win the competition for ZH_3 other than NH_3, for which the HB is comparable to the Br-bond. Within the subset of YH_2 bases, the XBs are considerably stronger for TeH_2, and HB is the clear winner for OH_2. For SH_2 and SeH_2, the HB is stronger than the ClB but weaker than both BrB and IB.

To examine basis set dependence, the interaction energies in the NH_3 and H_2O complexes were also recalculated at the MP2/aug-cc-pVTZ level (Table S1). It was found that the smaller basis set presents similar interaction energy to the larger one since their difference is less than 0.64 kcal mol^{-1}, corresponding to 3.0–7.2% of the MP2/aug-cc-pVDZ interaction energy. Thus the conclusions based on the MP2/aug-cc-pVDZ level are reliable.

2.2. Analysis of Wave Function

Partitioning of the total interaction energy into its constituent parts opens a window into the nature of the interaction. The interaction energies of HB and XB systems are decomposed here into five terms: electrostatic energy (E^{ele}), exchange energy (E^{ex}), repulsion energy (E^{rep}), polarization energy (E^{pol}) and dispersion energy (E^{disp}). All terms are given in Table S2, while only three attractive terms (E^{ele}, E^{pol}, and E^{disp}) are presented in Figure 3 for each of the complexes. In the HB interaction, E^{ele} is larger than E^{pol} and E^{disp}, indicating electrostatic interaction dominates the HB interaction, consistent with the parallel between E_{int} and V_{min} of the base. For the HB interaction with NH_3 and H_2O, E^{pol} is more negative than E^{disp}, while both terms are almost equal for the other ZH_3 and H_2Y. Clearly, the relative contribution of each term is related to the strength of the Lewis base. While decreasing the minimum MEP on the electron donor atom, E^{ele} also drops, as is also the case for E^{pol}. For the XB interactions, the electrostatic term is the largest but by only a narrow margin. In the bonds with YH_2, all three attractive terms grow as the Lewis base heavy atom becomes larger, but

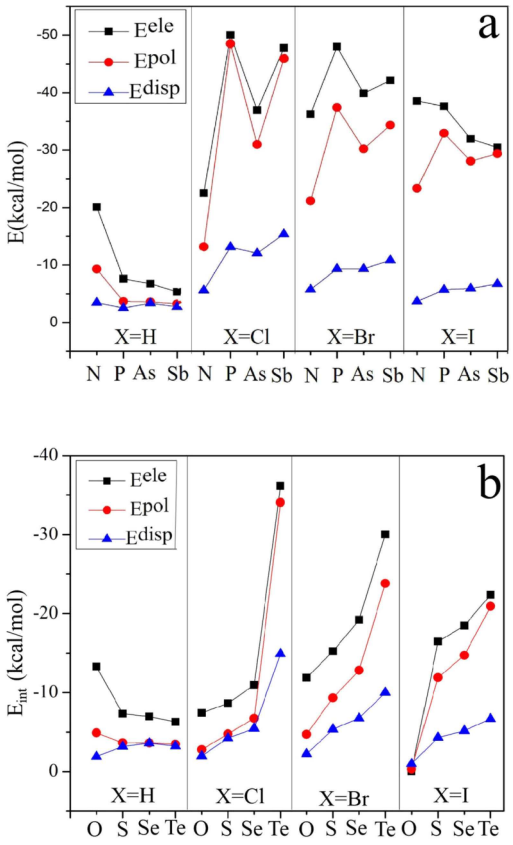

Figure 3. Electrostatic (E^{ele}), polarization (E^{pol}) and dispersion (E^{disp}) energies in complexes with a) ZH_3 and b) H_2Y.

the pattern is less clear for ZH_3, where there appears to be a minimum for AsH_3.

Another means of scrutinizing the interactions arises from an AIM analysis of the topology of the electron density. There is a bonding path leading from H/X to Y/Z in each complex, confirming the existence of a noncovalent bond. The most important properties of each bond critical point are reported in Table 2 where ρ refers to the density, $\nabla 2\rho$ to its Laplacian, and H is the energy density. The electron density ranges from 0.016 to 0.057 au, which lies in the range suggested for noncovalent interactions.[55] For the H-bonds, both ρ and $\nabla 2\rho$ decay as the Y/Z atom grows larger. The XBs obey a different patterns however. The Laplacian of the density is consistently largest for the smallest Y/Z atom, generally duplicating the HB trends. But the density behaves more erratically. ρ_{BCP} peaks for chalcogen atoms for fourth-row Te. But in the context of pnicogen electron donors, there is a predilection for P over the other atoms. H is quite small for most of these complexes, and of variable sign.

With respect to the particular flavor of halogen bond, neither ρ nor its Laplacian obeys a simple and clear pattern as one compares Cl with Br and I. As is commonly observed, an exponential relationship is present between the electron density at the bond critical point and the binding distance for the HB interactions, as may be seen in Figure S4. However,

Table 2. Electron density (ρ), Laplacian ($\nabla^2\rho$), and total energy density (H) at the intermolecular BCP in the HB and XB complexes (all values in a.u.).

	ρ	$\nabla^2\rho$	H		ρ	∇^2ρ	H
H-N	0.045	0.121	−0.002	Br-N	0.050	0.123	−0.005
H-P	0.020	0.039	0.001	Br-P	0.057	0.064	−0.012
H-As	0.019	0.035	−0.001	Br-As	0.049	0.060	−0.009
H-Sb	0.016	0.031	−0.001	Br-Sb	0.048	0.044	−0.009
H-O	0.032	0.141	0.005	Br-O	0.025	0.085	0.001
H-S	0.020	0.054	0.002	Br-S	0.027	0.068	0.001
H-Se	0.019	0.045	0.001	Br-Se	0.031	0.064	−0.001
H-Te	0.017	0.033	0.001	Br-Te	0.038	0.056	−0.004
Cl-N	0.040	0.121	0.001	I-N	0.047	0.108	−0.006
Cl-P	0.070	0.061	−0.018	I-P	0.046	0.063	−0.008
Cl-As	0.053	0.069	−0.009	I-As	0.041	0.055	−0.006
Cl-Sb	0.057	0.041	−0.013	I-Sb	0.038	0.040	−0.006
Cl-O	0.020	0.076	0.002	I-O	0.025	0.089	0.000
Cl-S	0.019	0.059	0.002	I-S	0.025	0.063	−0.000
Cl-Se	0.023	0.059	0.001	I-Se	0.027	0.058	−0.001
Cl-Te	0.051	0.059	−0.009	I-Te	0.030	0.048	−0.003

Table 3. Charge transfer (CT, in e) from Lewis acid to base molecule, and second-order perturbation energies (E^2, in kcal mol^{-1}) for transfer from Y/Z lone pair to O–H/O–X σ* antibonding orbital in the HB and XB complexes.

	CT	E^2		CT	E^2
H-N	0.056	39.16	Br-N	0.123	50.38
H-P	0.032	16.01	Br-P	0.272	88.07
H-As	0.030	14.11	Br-As	0.239	66.69
H-Sb	0.030	12.66	Br-Sb	0.302	74.92
H-O	0.026	21.24	Br-O	0.027	12.59
H-S	0.033	16.84	Br-S	0.082	25.76
H-Se	0.036	16.09	Br-Se	0.119	35.46
H-Te	0.037	15.02	Br-Te	0.232	66.99
Cl-N	0.078	28.60	I-N	0.126	54.28
Cl-P	0.347	106.01	I-P	0.227	78.29
Cl-As	0.246	61.84	I-As	0.209	63.12
Cl-Sb	0.412	93.53	I-Sb	0.245	63.94
Cl-O	0.016	6.82	I-O	0.039	19.22
Cl-S	0.040	11.93	I-S	0.102	33.87
Cl-Se	0.061	16.64	I-Se	0.133	41.20
Cl-Te	0.329	99.37	I-Te	0.200	58.77

there is no such relationship for the XB interactions, in keeping with some of the erratic patterns mentioned above.

Focus may be placed on charge transfer effects through an NBO analysis of the wave functions. The total charge transfer from Lewis acid to base molecule is reported in Table 3 as CT. This quantity displays some interesting patterns. First with regard to HBs, CT is largest for first-row N of the pnicogen donors, but smallest for first-row O. In the case of the XBs, there is a general tendency for larger charge transfer to the heavier electron donor atom: CT is more substantial for pnicogen than for chalcogen donors. This quantity is smaller for HBs than for XBs.

With respect to particular molecular orbitals, formation of any of these bonds is typically accompanied by transfer from the donor lone pair to the σ* antibonding OH or OX orbital. The energetic consequence of this transfer is measured as a second-order perturbation energy E^2 in the NBO formalism. These quantities in Table 3 only partially mirror the total intermolecular charge transfer CT. Both indicate that P is an anomalously strong electron donor, but only in halogen bonds. There is no such bump in these quantities for S as the second-row neighbor of P. Indeed, the chalcogen donors display an almost uniform increase in the charge transfer parameters as the Y atom grows in size. The same is true for the pnicogen donors, with the aforementioned anomaly for P. And like CT, E^2 tends to be larger for pnicogen than for chalcogen donors. Like the total intermolecular CT, E^2 tends toward larger values for the heavier Y/Z atoms, but this pattern is not universal, and a number of exceptions are present in Table 3.

For HBs, E^2 reflects consistently the change of the interaction energy, as evidenced by the linear relationship between both terms in Figure S5. This confirms the conclusion that HBs have a covalent contribution.[14] For the chalcogen donor if O is excluded, both E^2 and E_{int} display a linear variation in XBs. For the pnicogen donor, no linear relationship is found for both terms in XBs. When the chalcogen donor holds true and X varies from Cl to I, E_{int} increases for the stronger orbital interaction. Such change is also found for the XBs only when the N/Sb pnicogen donor is considered. The S chalcogen donor has larger E^2 value than the O analogue in XBs, but their interaction energies are almost equal. Similarly, for the P pnicogen donor, the interaction energies in the Cl and Br XBs are almost same although their corresponding orbital interaction has a big difference. This indicates that the stability of

some XBs cannot be explained only with electrostatic or orbital interactions.

2.3. Comparison with Previous Studies

Given some unexpected patterns in the data presented here, it would be worthwhile to compare our results with previous work in this arena. Our results first confirm the tight relationship between the strength of the H-bond and the basicity of the electron donor. There is a widely recognized increasing halogen bond strength in the Cl < Br < I sequence. While this trend is generally true here as well, anomalously strong Cl-bonds occur for the fourth-row atoms in the SbH_3 and H_2Te bases. There is some precedent for this apparent oddity. For example, the Cl-bond formed by ClF_5 with NH_3 is quite a bit stronger than the equivalent XBs formed by the Br and I analogues.[56] Huber et al had earlier observed unexpected trends in the strengths of halogen-bond dimers of CX_3I[57] wherein the XB strength ran counter to electronegativity of the substituent and to the intensity of the σ-hole. The authors ascribed this pattern to charge transfer/polarization which opposes simple Coulombic considerations. A similar explanation may be invoked here in that the CT and E^2 displayed in Table 3 for the Cl-bonds involving SbH_3 and H_2Te are surprisingly large.

With respect to the electron donors, the HB pattern closely fits the MEP minima in Figure 1. HB strengths diminish as the Y or Z atom moves down in the periodic table column. NH_3 forms a stronger HB than does H_2O, but it is the chalcogen that is a superior base for the second, third, and fourth row atoms, consistent with the Figure 1 data. But for the XBs, it is the pnicogen base which is uniformly stronger than its chalcogen counterpart in the same row of the periodic table, the reverse of the MEP trend. Again, this change in pattern can be traced to the charge transfer components in Table 3 where the pnicogen offers a stronger charge donor than does the chalcogen, with the exception of the first-row N and O atoms.

McDowell and Buckingham[58] considered the capacity of ClF to engage in a Cl-bond with bases similar to those examined here, but limited the latter to third-row atoms. Their interaction energies were consistently larger for ZH_3 than for YH_2, and by a sizable amount. As they progressed down either column of the periodic table, they observed a minimum interaction energy for second-row S and P atoms, counter to conventional wisdom. However, these trends change, and become less regular, upon replacement of H atoms on the base by methyl groups. For example, whereas the ClB to the chalcogen base rises regularly O < S < Se, the pattern for the pnicogen leads to the largest interaction energy for the second-row P.

Taking under consideration some of the irregular patterns noted here, in conjunction with certain anomalies noted by others in related systems, it would seem that the origin of the halogen bond should be comprehensively elucidated by a combination of electrostatic and orbital interactions. Further study on base of orbital interactions is needed to fully unravel some of these issues, which reside in the properties of both the Lewis acid and base. The Cl–Te complex has greater stability than the other Cl-chalcogen analogues in spite of the smallest negative MEP on the Te atom. This abnormal result can be explained with the orbital interaction since it is strongest in the Cl–Te complex. A similar reason is also responsible for the largest interaction energy in the Br–Te and I–Te complexes. The larger interaction energy in the Cl–P complex relative to that in the Cl–N complex is also ascribed to the presence of a strong orbital interaction.

3. Conclusions

The HBs formed by 6-OH-fulvene are generally weaker than its XBs. Halogen bonds to pnicogen ZH_3 molecules are stronger than those involving chalcogen YH_2 units. The XB strength grows along with the size of the halogen atom, but the dependence upon donor atom size is less clear. The fourth-row Te atom offers the strongest XBs to chalcogen donors, whereas it is the smallest N pnicogen atom that provides the strongest XB (with an exception for the Cl···Sb bond which is surprisingly strong). The largest contributor to most of these bonds is the electrostatic attraction, but polarization energy does not lag far behind. Neither the total interaction energy, nor its electrostatic component, is strictly proportional to the value of the minimum in the electrostatic potential surrounding the electron donor molecule. Of the various binary complexes considered here, the strongest involves a I···N XB with an interaction energy of −15.6 kcal mol^{-1}. The weakest interaction occurs in the HB to a pnicogen Sb atom.

Acknowledgements

This work was supported by the National Natural Science Foundation of China (21573188).

Conflict of Interest

The authors declare no conflict of interest.

Keywords: AIM · charge transfer · energy decomposition · molecular electrostatic potential · NBO

[1] S. Scheiner, *Hydrogen Bonding: A Theoretical Perspective*, Oxford University Press, New York, **1997**.
[2] a) C. B. Aakerçy, M. Baldrighi, J. Desper, P. Metrangolo, G. Resnati, *Chem. Eur. J.* **2013**, *19*, 16240–16247; b) R. W. Troff, T. Mäkelä, F. Topić, A. Valkonen, K. Raatikainen, K. Rissanen, *Eur. J. Org. Chem.* **2013**, 1617–1637.
[3] R. F. W. Bader, *Atoms in molecules: A quantum theory*, Oxford University Press, Oxford. **1990**.
[4] G. A. Jeffrey, *An Introduction to Hydrogen Bonding*, Oxford University Press, New York, **1997**.
[5] S. Scheiner, *Noncovalent Forces*, Spinger, **2015**.
[6] G. R. Desiraju, T. Steiner, *The Weak Hydrogen Bond*, Oxford University Press, Oxford, U. K., **1999**.

[7] L. C. Gilday, T. Lang, A. Caballero, P. J. Costa, V. Felix, P. D. Beer, *Angew. Chem. Int. Ed.* **2013**, *52*, 4356–4360; *Angew. Chem.* **2013**, *125*, 4452–4456.
[8] A. V. Jentzsch, S. Matile, *J. Am. Chem. Soc.* **2013**, *135*, 5302–5303.
[9] H. R. Khavasi, A. A. Tehrani, *Inorg. Chem.* **2013**, *52*, 2891–2905.
[10] J. E. Ormond-Prout, P. Smart, L. Brammer, *Cryst. Growth Des.* **2012**, *12*, 205–216.
[11] H. S. El-Sheshtawy, B. S. Bassil, K. I. Assaf, U. Kortz, W. M. Nau, *J. Am. Chem. Soc.* **2012**, *134*, 19935–19941.
[12] L. Meazza, J. A. Foster, K. Fucke, P. Metrangolo, G. Resnati, J. W. Steed, *Nat. Chem.* **2013**, *5*, 42–47.
[13] T. Clark, M. Hennemann, J. S. Murray, P. Politzer, *J. Mol. Model.* **2007**, *13*, 291–296.
[14] L. P. Wolters, F. M. Bickelhaupt, *ChemistryOpen.* **2012**, *1*, 96–105.
[15] B. Domercq, T. Devic, M. Fourmigué, P. Auban-Senzier, E. Canadell, *J. Mater. Chem.* **2001**, *11*, 1570–1575.
[16] H. M. Yamamoto, Y. Kosaka, R. Maeda, J. Yamaura, A. Nakao, T. Nakamura, R. Kato, *ACS Nano* **2008**, *2*, 143–155.
[17] H. M. Yamamoto, J. Yamaura, R. Kato, *J. Am. Chem. Soc.* **1998**, *120*, 5905–5913.
[18] A. Matsumoto, T. Tanaka, T. Tsubouchi, K. Tashiro, S. Saragai, S. Nakamoto, *J. Am. Chem. Soc.* **2002**, *124*, 8891–8902.
[19] A. Farina, S. V. Meille, T. M. Messina, P. Metrangolo, G. Resnati, G. Vecchio, *Angew. Chem. Int. Ed.* **1999**, *38*, 2433–2436; *Angew. Chem.* **1999**, *111*, 2585–2588.
[20] F. Wang, N. Ma, Q. Chen, W. Wang, L. Wang, *Langmuir.* **2007**, *23*, 9540–9542.
[21] P. Auffinger, F. A. Hays, E. Westhof, P. S. Ho, *Proc. Natl. Acad. Sci. USA* **2004**, *101*, 16789–16794.
[22] A. R. Voth, H. P. Shing, *Cur. Top. Med. Chem.* **2007**, *7*, 1336–1348.
[23] J. Lieffrig, O. Jeannin, T. Guizouarn, P. Auban-Senzier, M. Fourmigué, *Cryst. Growth Des.* **2012**, *12*, 4248–4257.
[24] H. Duan, W. Zhang, J. Zhao, D. Liang, X. Yang, S. Jin, *J. Mol. Model.* **2012**, *18*, 3867–3875.
[25] C. B. Aakerçy, J. Desper, B. A. Helfrich, P. Metrangolo, T. Pilati, G. Resnati, A. Stevenazzi, *Chem. Commun.* **2007**, *41*, 4236–4238.
[26] C. B. Aakerőy, T. K. Wijethunga, J. Desper, M. Đaković, *Cryst. Growth Des.* **2016**, *16*, 2662–2670.
[27] T. Clark, *Faraday Discuss.* **2017**, *203*, 9–27.
[28] M. D. Perera, J. Desper, A. S. Sinha, C. B. Aakeröy, *CrystEngComm.* **2016**, *18*, 8631–8636.
[29] R. K. Rowe, P. S. Ho, *Acta. Crystallogr. Sect. B: Struct. Sci. Cryst. Eng. Mater.* **2017**, *73*, 255–264.
[30] C. A. Gunawardana, J. Desper, A. S. Sinha, M. Đaković, C. B. Aakeröy, *Faraday Discuss.* **2017**, *203*, 371–388.
[31] C. B. Aakeröy, P. D. Chopade, J. Desper, *Cryst. Growth Des.* **2011**, *11*, 5333–5336.
[32] H. R. Khavasi, A. A. Tehrani, *CrystEngComm.* **2013**, *15*, 5813–5820.
[33] D. A. Adsmond, A. S. Sinha, U. B. R. Khandavilli, A. R. Maguire, S. E. Lawrence, *Cryst. Growth Des.* **2016**, *16*, 59–69.
[34] T. Shirman, M. Boterashvili, M. Orbach, D. Freeman, L. J. W. Shimon, M. Lahav, M. E. van der Boom, *Cryst. Growth Des.* **2015**, *15*, 4756–4759.
[35] H. R. Khavasi, M. Esmaeili, *CrystEngComm.* **2014**, *16*, 8479–8485.
[36] P. Metrangolo, G. Resnati, *Science* **2008**, *321*, 918–919.
[37] C. C. Robertson, J. S. Wright, E. J. Carrington, R. N. Perutz, C. A. Hunter, L. Brammer, *Chem. Sci.* **2017**, *8*, 5392–5398.
[38] H. L. Xu, Q. Z. Li, S. Scheiner, *ChemPhysChem.* **2018**, *19*, 1456–1464.
[39] N. Nagels, Y. Geboes, B. Pinter, F. D. Proft, W. A. Herrebout, *Chemistry* **2014**, *20*, 8433–8443.
[40] Y. Geboes, F. D. Proft, W. A. Herrebout, *J. Mol. Struct.* **2018**. *1165*, 349–355
[41] X. L. An, H. Y. Zhuo, Y. Y. Wang Y. Q. Z. Li, *J. Mol. Model.* **2013**, *19*, 4529–4535.
[42] X. L. An, X. Yang, B. Xiao, J. B. Cheng, Q. Z. Li, *Mol. Phys.* **2017**, *115*, 1614–1623.
[43] K. J. Stone, R. D. Little, *Chem. Informationsdienst* **1984**, *15*, 1849–1853.
[44] A. J. Peloquin, R. L. Stone, S. E. Avila, *J. Org. Chem.* **2012**, *77*, 6371–6376.
[45] K. Strohfeldt, M. Tacke, *Chem. Soc. Rev.* **2008**, *37*, 1174–1187.
[46] S. Noorizadeh, E. Shakerzadeh, *Comput. Theor. Chem.* **2011**, *964*, 141–147.
[47] M. J. Frisch, G. W. Trucks, H. B. Schlegel, G. E. Scuseria,M. A. Robb, J. R. Cheeseman, G. Scalmani, V. Barone, B. Mennucci, G. A. Petersson, H. Nakatsuji, M. Caricato,X. Li, H. P. Hratchian, A. F. Izmaylov, J. Bloino, G. Zheng, J. L. Sonnenberg, M. Hada, M. Ehara, K. Toyota, R. Fukuda, J. Hasegawa, M. Ishida, T. Nakajima, Y. Honda, O. Kitao, H. Nakai, T. Vreven, J. J. A. Montgomery, J. E. Peralta, F. Ogliaro, M. Bearpark, J. J. Heyd, E. Brothers, K. N. Kudin, V. N. Staroverov, R. Kobayashi, J. Normand, K. Raghavachari, A. Rendell, J. C. Burant, S. S. Iyengar, J. Tomasi, M. Cossi, N. Rega, J. M. Millam, M. Klene, J. E. Knox, J. B. Cross, V. Bakken, C. Adamo, J. Jaramillo, R. Gomperts, R. E. Stratmann, O. A. Yazyev, J. Austin, R. Cammi, C. Pomelli, J. W. Ochterski, R. L. Martin, K. Morokuma, V. G. Zakrzewski, G. A. Voth, P. Salvador, J. J. Dannenberg, S. A. Dapprich, D. Daniels, O. Farkas, J. B. Foresman, J. V. Ortiz, J. Cioslowski, D. J. Fox, Gaussian 09, Revision A.02, Gaussian, Inc. Wallingford, CT, **2009**.
[48] S. F. Boys, F. Bernardi, *Mol. Phys.* **1970**, *19*, 553–556.
[49] A. E. Reed, L. A. Curtiss, F. Weinhold, *Chem. Rev.* **1988**, *88*, 899–926.
[50] R. F. W. Bader, AIM2000 Program, v. 2.0, McMaster University, Hamilton, Canada, **2000**.
[51] F. A. Bulat, A. Toro-Labbe, T. Brinck, J. S. Murray, P. Politzer, *J. Mol. Model.* **2010**, *16*, 1679–169
[52] P. F. Su, H. Li, *J. Chem. Phys.* **2009**, *131*, 014102.
[53] M. W. Schmidt, K. K. Baldridge, J. A. Boatz, S. T. Elbert, M. S. Gordon, J. H. Jensen, S. Koseki, N. Matsunaga, K. A. Nguyen, S. J. Su, T. L. Windus, M. Dupuis, J. A. Montgomery, *J. Comput. Chem.* **1993**, *14*, 1347–1363.
[54] Q. Z. Li, R. Li, S. C. Yi, W. Z. Li, J. B. Cheng, *Struct. Chem.* **2012**. *23*, 411–416.
[55] P. Lipkowski, S. J. Grabowski, T. L. Robinson, J. Leszczynski, *J. Phys. Chem. A* **2004**, *108*, 10865–10872.
[56] S. Scheiner, J. Lu, *Chem. Eur. J.* **2018**, *24*, 8167–8177.
[57] S. M. Huber, E. Jimenez-Izal, J. M. Ugalde, I. Infante, *Chem. Commun.* **2012**, *48*, 7708–7710.
[58] S. A. C. McDowell, A. D. Buckingham, *ChemPhysChem.* **2018**, *19*, 1756–1765.

Manuscript received: April 7, 2019
Revised manuscript received: May 28, 2019
Accepted manuscript online: May 29, 2019
Version of record online: June 21, 2019